Am J Transl Res 2017;9(6):3060-3072
www.ajtr.org /ISSN:1943-8141/AJTR0049800

Original Article

Chronic intermittent hypoxia decreases pulmonary clearance of ^{99m}Tc-labelled particulate matter in mice

Cuiping Fu[1*], Huan Lu[1*], Xu Wu[1*], Jie Liu[1], Chengying Liu[2], Zilong Liu[1], Wei Yuan[3], Jian Zhou[1], Shanqun Li[1]

[1]Department of Pulmonary Medicine, Center of Snoring and Sleep Apnea Medicine, Zhongshan Hospital of Fudan University, Shanghai 200032, China; [2]Department of Respiratory Medicine, Affiliated Jiangyin Hospital of Southeast University, Jiangyin 214400, China; [3]Department of Pathology Medicine, Zhongshan Hospital of Fudan University, Shanghai 200032, China. [*]Equal contributors and co-first authors.

Received January 28, 2017; Accepted May 18, 2017; Epub June 15, 2017; Published June 30, 2017

Abstract: Background: Obstructive sleep apnea-hypopnea syndrome (OSAHS) could cause systematic inflammation including pulmonary inflammatory response, whereas the influence of OSAHS in pulmonary clearance ability remains unknown. The main pathophysiological feature of OSAHS is chronic intermittent hypoxia (CIH). The goal of this study is to clarify the airway clearance of particulate matter (PM) in CIH mice, and to explore the potential mechanism. Methods: Balb/c mice were divided into a CIH group and a control group, exposed to intermittent hypoxia and air chamber, respectively. A radioactive probe, ^{99m}Tc labeled PM, was endotracheally inserted into the mice at 10 mg/kg, with a starting dose of 800 μCi. The change of radioactive dose reserved in the lung was observed using single-photon emission computed tomography/computed tomography (SPECT/CT) and reconstructed data were analyzed. Special airway resistance (sRaw) of mice was measured by non-invasive airway mechanics sites. Lung resistive load (R_L), elastic resistance, and compliance were measured by a multichannel physiological signal system. Lung injury was judged by hematoxylin-eosin staining and histologic score. Change in mucus secretion was determined using periodic acid-Schiff staining and enzyme-linked immunosorbent assay. Fresh lung tissue was used for real-time polymerase chain reaction and western blot analysis to explore related change of inflammation and signaling molecules and potential mechanical pathway. Results: Mice in the CIH group had higher PM radioactive deposit than the control group (93.37±3.44 μCi vs. 65.98±2.61 μCi). The average radiation dose in the lung was elevated (0.0005 μCi/mm^3 vs. 0.0001383 μCi/mm^3). Mice in the CIH group have higher value of sRaw, R_L, and elastic resistance, whereas pulmonary compliance decreased compared to the control group (2.13±0.29 mL/cmH_2O vs. 5.37±1.02 mL/cmH_2O). The CIH group showed a higher histopathological score. Several genes associated with mucin secretion such as chemokine (C-X-C motif) ligand 1 (CXCL1), Clara Cell Secretory Protein 16 (CC16), macrophage inflammatory protein 2 (MIP-2), chloride channel regulator 1 (Gob5), and mucin 5AC (MUC5AC) showed elevated expression. Phosphatidylinostol-3-kinase/serine/threonine-specific protein kinase (PI3K/AKT) pathway was activated in the CIH group. Conclusions: CIH decreased pulmonary clearance of PM and increased lung airway resistance, which may be related to inflammatory response and mucus hypersecretion in the lung.

Keywords: Intermittent hypoxia, particulate matter, clearance, mucin, airway resistance

Introduction

Particulate matter (PM) in air pollution, a mixture of solid particles and liquid droplets existing in the air, exerts a negative effect on human health. There is growing concern that long-term exposure to ambient airborne PM is associated with various respiratory diseases [1]. The metal content, the presence of polycyclic aromatic hydrocarbons (PAHs) and other organic components such as endotoxins, mainly contribute to PM toxicity [2]. Despite extensive research on the adverse effects of air pollution on human health, little is known about the effect of air pollution on obstructive sleep apnea-hypopnea syndrome (OSAHS), which leads to chronic intermittent hypoxia (CIH) during sleep [3]. Apnea-hypopnea index was significantly associated with race and environmental tobacco smoke, highlighting the potential effect of environmental factors [4]. The recurrent episodic disruption of normal breathing during sleep was shown to be related to air pollution, and may be more prevalent in poor urban environments [5].

OSAHS and air pollution have each been linked to increased risk of autonomic dysfunction, and pulmonary and systemic inflammation [6, 7]. However, the specific influence of pollution on OSAHS is poorly understood.

Mucociliary transport is one of the major ways for PM to be removed from ambient air [8]. Initially, ambient air is filtered by the nose with deposition of PM on nasal hairs and mucosa due to rheologic effects. There is continuing particulate impaction at turns or bifurcations in the airways, with sedimentation in gelations in the airways and in gelatinous mucus. This suggested that airway inflammation and the condition of mucus secretion affected the clearance of PM. Studies have shown that CIH usually develops as a result of both systematic and local inflammation [9]. Patients with OSAHS can be more likely to suffer inflammatory response or immune injury [10]. Mucociliary clearance (MCC) is an essential innate defense mechanism that continuously removes inhaled pathogens and particulates from the airway. Normal MCC is important for maintaining a healthy respiratory system, and impaired MCC is a feature of many airway diseases [11]. Mucus hypersecretion is a direct reason for disabled MCC. In addition, increased airway resistance could affect the pulmonary clearance ability [12]. Currently, the pulmonary clearance ability in OSAHS patients has not been explored clearly. Although inflammation response in OSAHS patients has been studied in recent years, the change of mucus secretion and pulmonary airway resistance is less understood. Therefore, the aim of our study is to clarify the airway clearance ability in mice with intermittent hypoxia, and to explore the potential mechanism.

We developed a mouse model of CIH, which mimicked oxyhemoglobin desaturations in patients with OSAHS [13], to explore its effects on airway clearance ability and pulmonary clearance function of PM and to explore the potential mechanism. In this study, we focused on mucus secretion and airway resistance in decreasing pulmonary clearance of PM.

Methods

Experimental animals

The animals were weighed and randomly divided into two groups. One group was exposed to CIH. The other group was exposed to air and used as a control. An established rodent model of CIH was utilized [14]. Briefly, CIH mice were placed into a specially designed chamber, which contained a gas control delivery system to regulate the flow of oxygen and nitrogen into the chamber. During each 1-minute period of intermittent hypoxia, the oxygen concentration in the chamber was adjusted between 7% and 21%. Nitrogen was introduced at a rate sufficient to achieve a fraction of inspired oxygen (FiO_2) of 7% within 30 seconds and to maintain this level of FiO_2 for 10 seconds; then, oxygen was introduced at a rate to achieve a FiO_2 of 21% within 20 seconds. Balb/C mice were placed into this chamber for 9 hours daily, 7 days per week, for 6 consecutive weeks. At all other times, the mice were kept in chambers with an oxygen concentration of 21%. The oxygen concentration in these chambers was continuously observed by an oxygen analyzer, and the levels were under feedback control by a computerized system connected to a gas valve outlet. Deviation from the determined settings was corrected by the addition of pure nitrogen or oxygen through solenoid valves. The control group was handled in the same manner as the CIH group, except oxygen concentration in the control chambers was maintained at a constant 21% throughout the experiment. Mice were purchased from the Fudan University animal center and were maintained on a 12:12-hour night-day cycle, with standard mice chow and water available ad libitum. The experimental protocol was approved by the local Animal Care and Use Committee of Fudan University.

^{99m}Tc-labelled-DTPA-PM

PM (Urban dust NIST® SRM® 1649B, Sigma) standard reference material was used in this study, available from the National Institute of Standards and Technology (NIST), containing selected PAHs, nitro-substituted PAHs (nitro-PAHs), polychlorinated biphenyl congeners, chlorinated pesticides, and inorganic constituents in atmospheric particulate material and similar matrices. ^{99m}Tc labeling diethylenetriaminepentaacetic acid (DTPA, Sigma, USA) was conjugated to PM following the established similar protocol [15]. Briefly, synthesis of condenses of DTPA with PM: 100 μg PM was added in a 30-k tube, and then DTPA was added to the tube, shaking for 1 hour on a swag bed at room temperature. Next, a solution of ammonium

acetate (0.25 M) was added to the tube, and extra DTPA was removed after centrifugation.

DTPA-PM was then labeled with ^{99m}Tc following the developed method [16]. DTPA-PM conjugate was added to the equal volume of labeling buffer, and then (around 1 mCi) $Na^{99m}TcO4$ was added. Immediately after vortexing, 3 μL freshly prepared 1 mg/mL $SnCl_2{\cdot}2\ H_2O$ solution was added. The combined solution was incubated at room temperature for 1 hour under vortexing. ^{99m}Tc-DTPA-PM was instilled intratracheally into mice with a dose of 250 μg/800 μCi/mouse.

Micro-single-photon emission computed tomography/computed tomography and imaging analysis

Balb/C mice (male, 8 weeks) received ^{99m}Tc-DTPA-PM. One hour later, mice were anesthetized via 2% isoflurane inhalation. Computed tomography (CT) was performed first with the following parameters: frame resolution, 256 × 512; tube voltage, 45 kVp; current, 0.15 mA; and exposure time, 500 ms/frame. Each scan took about 8 minutes. Single-photon emission computed tomography (SPECT) was performed after CT with the same bed position using the following parameters: four high-resolution conical collimators with nine-pinhole plates; energy peak, 140 keV; window width, 10%; resolution, 1 mm/pixel; matrix, 256 × 256; and scan time, 35 s/projection, 24 projections in all. Each mouse took 21 minutes on average. Three-dimensional ordered subset expectation maximization images were reconstructed using HiSPECT algorithm. Two hours after instillation, each mouse was repeated above operation. Reconstructed SPECT/CT data were transferred to software InVivoScope (Version 1.43, Bioscan, Washington DC, USA) for post-processing. Concentration of radioactivity (μCi/mm^3) was automatically generated by the software for each region of interest (ROI).

Airway resistance detection

Specific airway resistance (sRaw) in the conscious mice was assessed by FinePointe™ Non-Invasive Airway Mechanics sites (Buxco Electronics, Inc., Wilmington, North Carolina) according to a previously reported method [17]. This site used double-flow plethysmography that calculated sRaw by analyzing breathing patterns at nasal and thoracic airflows. For the determination of sRaw in mice, inhalations of saline and methacholine were administered. Aerosols were delivered into the nasal cavity for 1 minute in a dose-response manner: 0 (saline), 3.125, 6.25, 12.5, 25, and 50 mg of methacholine per milliliter. The reliability and reproducibility of measurements made using noninvasive double-flow plethysmography were increased by ensuring that all measurements were made in an air-conditioned environment controlled for temperature (22°C to 23°C) and humidity (50% to 60%). In addition, airway resistance including pulmonary compliance, pulmonary R_L, and pulmonary elastic resistance was measured by a RM6240 multichannel physiological signal system (Chengyi, China) based on the methods described by Strope et al [18] and Amdur et al [19].

Methods to explore the change of mucus secretion

Bronchoalveolar lavage fluid was collected for enzyme-linked immunosorbent assay for the detection of Mucin 5AC (MUC5AC, Cusabio Biotech Co. Wuhan, China). MUC5AC expression was measured following the instructions provided in the enzyme-linked immunosorbent assay kit. Lung tissues were removed from mice after anesthesia and filled with 10% buffered formalin, and then were embedded in paraffin and 5 mm sections were cut for hematoxylin and eosin staining and periodic acid-Schiff (PAS) staining. In addition, other parts of the lung were stored at -80°C for ribonucleic acid (RNA) and protein extraction. Related signaling molecules and potential mechanical pathway were explored by real-time polymerase chain reaction and western blot analysis.

PAS is a common carbohydrate stain, which in the lung reveals mucin-secreting cells because mucins are very rich in glycans. Histologic sections were stained with PAS (Sigma-Aldrich, USA) followed by standard protocols as previously described [20]. Double-blind analysis of integrated optical density of mucin granules in large and small airways was performed using Image-Pro Plus 6.0.

Lung histology evaluation

According to a lung injury scoring method previously proposed [21], the degree of microscopic

injury was quantified based on the following: alveolar and interstitial edema, inflammatory infiltration, and hemorrhage. The severity of injury was graded for each variable: no injury = 0; injury to 25% of the field = 1; injury to 50% of the field = 2; injury to 75% of the field = 3; and diffuse injury = 4. All hematoxylin and eosin slides were analyzed by a pathologist who was blinded to the study. A total of three slides from each lung sample were randomly screened and the mean was taken as the representative value of the sample.

Real-time polymerase chain reaction

Total RNA (ThermoFisher Scientific Ambion, USA) was extracted from the pulmonary cells in each group using trizol reagent (Life Technologies). The extraction was verified by electrophoresis on 1.0% agarose gel and an absorbance (A260/280) value of 1.8-2.0. Reverse transcription for complementary deoxyribonucleic acid was performed using a real-time polymerase chain reaction kit. Expression of β-actin, MUC5AC, chemokine (C-X-C motif) ligand 1 (CXCL1), macrophage inflammatory protein 2 (MIP-2), chloride channel regulator 1 (CLCA1 namely Gob5), phosphoinositide 3-kinase (PI3K) and Clara Cell Secretory Protein 16 (CC16) was measured. The polymerase chain reaction primers are listed as follows:

β-actin: 5'-GTACCACCATGTACCCAGGC-3' (forward); 5'-AACGCAGCTCAGTAACAGTCC-3' (reverse). MUC5AC: 5'-CCCTTTCCGATGTCTTTATGGT-3' (forward); 5'-GCCTGGTACTCAGAGCCCTTAG-3' (reverse). Gob5: 5'-TACATAGATGGCTGGATTGAGG-3' (forward); 5'-CAGTGATTTGACAGGGTGGAA-3' (reverse). MIP-2: 5'-GCCCAGACAGAAGTCATAGCC-3' (forward); 5'-CTCCTCCTTTCCAGGTCAGTT-3' (reverse). CXCL1: 5'-ACCCAAACCGAAGTCATAGCC-3' (forward); 5'-AGAAGCCAGCGTTCACCAGA-3' (reverse). CC16: 5'-GGCATTGTCACCCACTTTC-3' (forward); 5'-CTCCAGATGGCTCTAACCG-3' (forward). PI3K: 5'-CTGAGTTTGTTTCTGGGGTTCC-3' (forward); 5'-CTGAGTTTGTTCTGGGGTTCC-3' (reverse).

The polymerase chain reactions were carried out as follows: a predenaturing at 95°C for 5 minutes, followed by 30 cycles of denaturation at 95°C for 30 seconds, annealing at 58°C for 40 seconds, and extension at 72°C for 45 seconds. Polymerase chain reaction products were separated by electrophoresis through 1% agarose gel containing ethidium bromide, and the signal intensity was analyzed using Quantity One software.

Western blot analysis

The cells were lysed in a radioimmunoprecipitation assay lysis buffer with protease inhibitor and phosphatase inhibitor. Equal amounts of cell lysate from the protein samples were resolved by 10% and 12% sodium dodecyl sulfate-polyacrylamide gel electrophoresis and transferred onto polyvinylidene difluoride membranes. These membranes were incubated with 5% bovine serum albumin in phosphate buffered saline Tween at room temperature for and exposed to specific primary antibodies against reduced glyceraldehyde-phosphate dehydrogenase (GAPDH, Cell Signaling Technology), PI3K (Cell Signaling Technology), phosphorylates-PI3K (P-PI3K, P85, Cell Signaling Technology), serine/threonine-specific protein kinase (AKT, Cell Signaling Technology) and phosphorylates-AKT (P-AKT, Thr308, Cell Signaling Technology, at 1:1000) overnight at 4°C. This was then followed by incubation with horseradish peroxidase-conjugated goat anti-mouse and anti-rabbit secondary antibodies (Abcam, USA, at 1:4000) for 2 hours at room temperature [22]. The blots were visualized by enhanced chemiluminescence. The intensity of each band was measured using Quantity One software. The relative protein expression level was determined by normalization to expression of GAPDH.

Statistical analysis

Data were analyzed using Pearson correlation coefficient with SPSS 17.0 software (SPSS, Inc., Chicago, IL, USA) and are presented as the means ± standard deviation. The data were also analyzed using the Student *t*-test. *P*-values <0.05 were considered to indicate statistically significant differences.

Results

CIH mice increased radioactive deposit in the lung

The radiolabeling yield of ^{99m}Tc-labeled PM was over 95%. Equal radiological dose of ^{99m}Tc-labeled PM was ensured to be instilled into the trachea of mice, according to the fixed radioac-

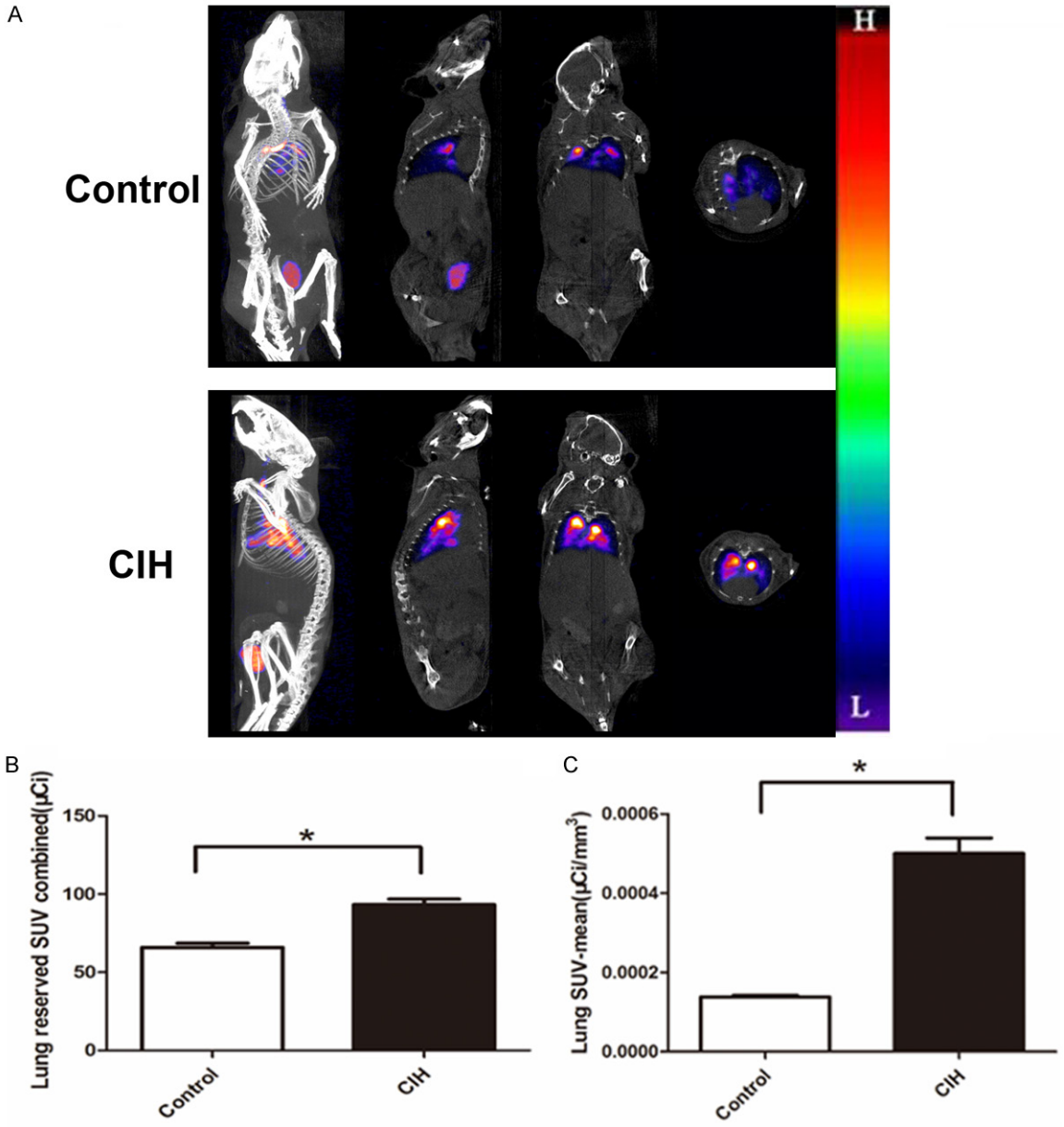

Figure 1. Mice with CIH had increased radioactive deposit in the lungs. N=6 per group. A. Single-photon emission computed tomography/computed tomography showed the reconstruction, coronal, sagittal, and transverse sections (from left to right) in the control (the upper images) and CIH groups (the lower images). The color from "L" to "H" indicate radioactivity accumulation from low to high. B. Lung reserved SUV sum in the lung in the CIH group and the control group (P=0.011). C. Lung SUV-mean value in two groups (P=0.006). Data represent three independent experiments. All data were analyzed by SPSS using independent-sample *t*-test.

tive decay formula. The micro-SPECT/CT imaging showed a significant overall increased pulmonary reserved radioactivity over time in the CIH group mice (**Figure 1A**) and the animated images in GIF format of the control and CIH group are shown in Figures S1 and S2, respectively. Mice in the CIH group had higher PM radioactive deposit than the control group (89.6465 μCi vs. 65.9811 1 μCi) 1 hour after instillation (P<0.05, **Figure 1B**). The average radiation dose in the lung was elevated (0.06927 μCi/mm^3 vs. 0.00014 μCi/mm^3, P<0.05, **Figure 1C**). Furthermore, the same condition extended to 2 hours after instillation (data not shown).

CIH increased airway resistance

sRaw was measured as an indicator of airway resistance and was different from the control

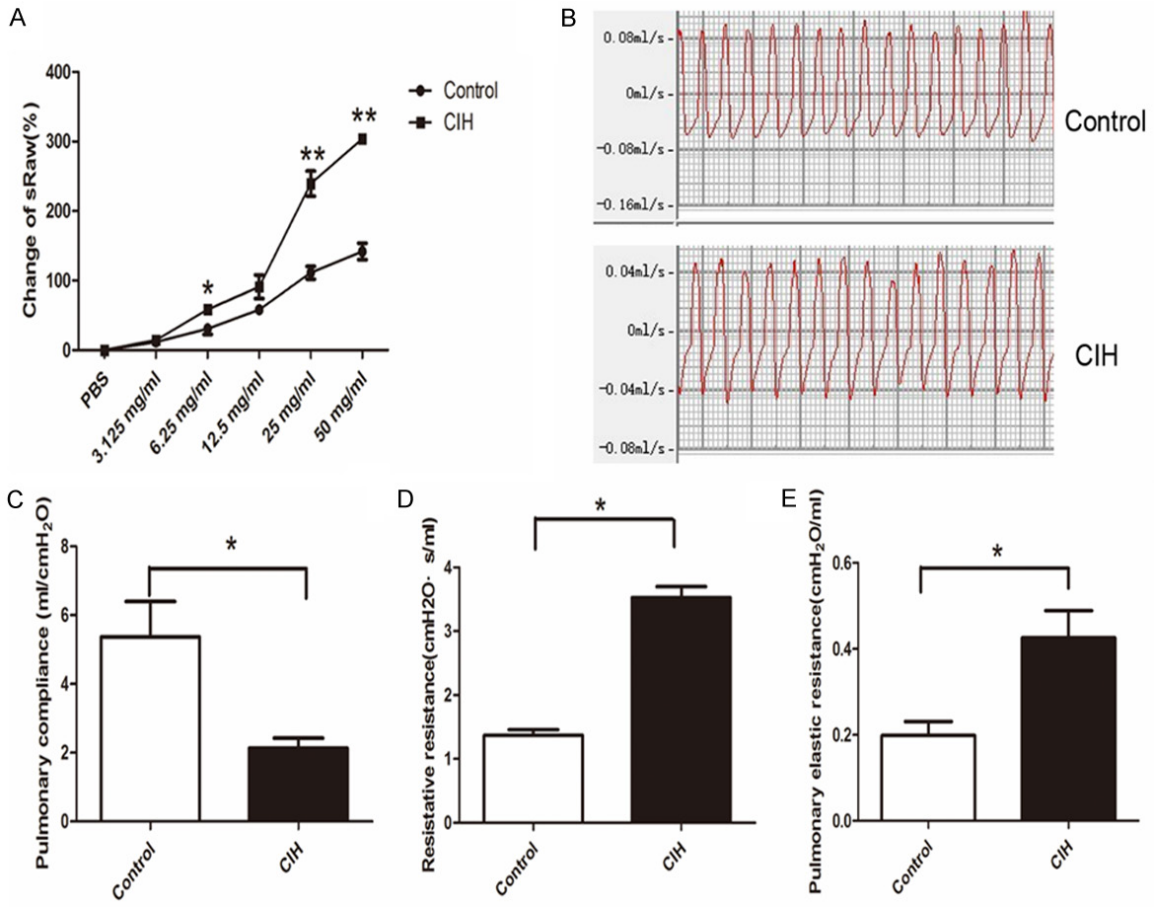

Figure 2. CIH increased airway resistance. N=6 per group. A. Change of sRaw curve in each stimulation point in two groups. Significant difference shown in 6.25 mg/mL, 25 mg/mL, and 50 mg/mL stimulation points (P<0.05). B. Respiratory wave in control and CIH groups. Mice with CIH showed lower respiratory flow, nearly 0.04 mL/s, compared to the control mice (0.08 mL/s). C. Pulmonary compliance statistical graph of two groups (P=0.038). D. Resistive resistance in two groups (P=0.0004). E. Pulmonary elastic resistance in two groups (P=0.0336). Data represent three independent experiments. All data were analyzed by SPSS using independent-sample *t*-test.

group. The value of sRaw (cm H_2O × s) after aerosolizing different concentrations of methacholine was significantly increased in the CIH group compared to that of the control group. **Figure 2A** shows the percentage change of sRaw value in the CIH group was significantly higher at 6.25 mg/mL, 25 mg/mL, and 50 mg/mL (P<0.05). **Figure 2B** displayed the schematic respiratory wave in the control and CIH groups. CIH mice showed lower respiratory flow, nearly 0.04 mL/s, compared to the control mice (0.08 mL/s). Measurement of invasive ventilation parameter showed that the pulmonary compliance decreased in the CIH group (P<0.05, **Figure 2C**, whereas the pulmonary resistive resistance (R_L) and elastic resistance increased compared to the control group (P<0.05, **Figure 2D**, **2E**). Furthermore, minute ventilation, intrapleural pressure, and respiratory rate had no obvious change (data not shown). These results indicated that both special airway resistance and pulmonary ventilation resistance were higher after CIH exposure.

Lung inflammatory response and mucus hypersecretion in mice with CIH

Histological examination of lung tissues was further performed. The results showed more severe damage in the lung of CIH mice than the control, assessed by the change of alveolar and interstitial edema, hemorrhage, and the infiltration of inflammatory cells (**Figure 3A**). We further evaluated the histological score and found it was significantly higher in mice in the CIH

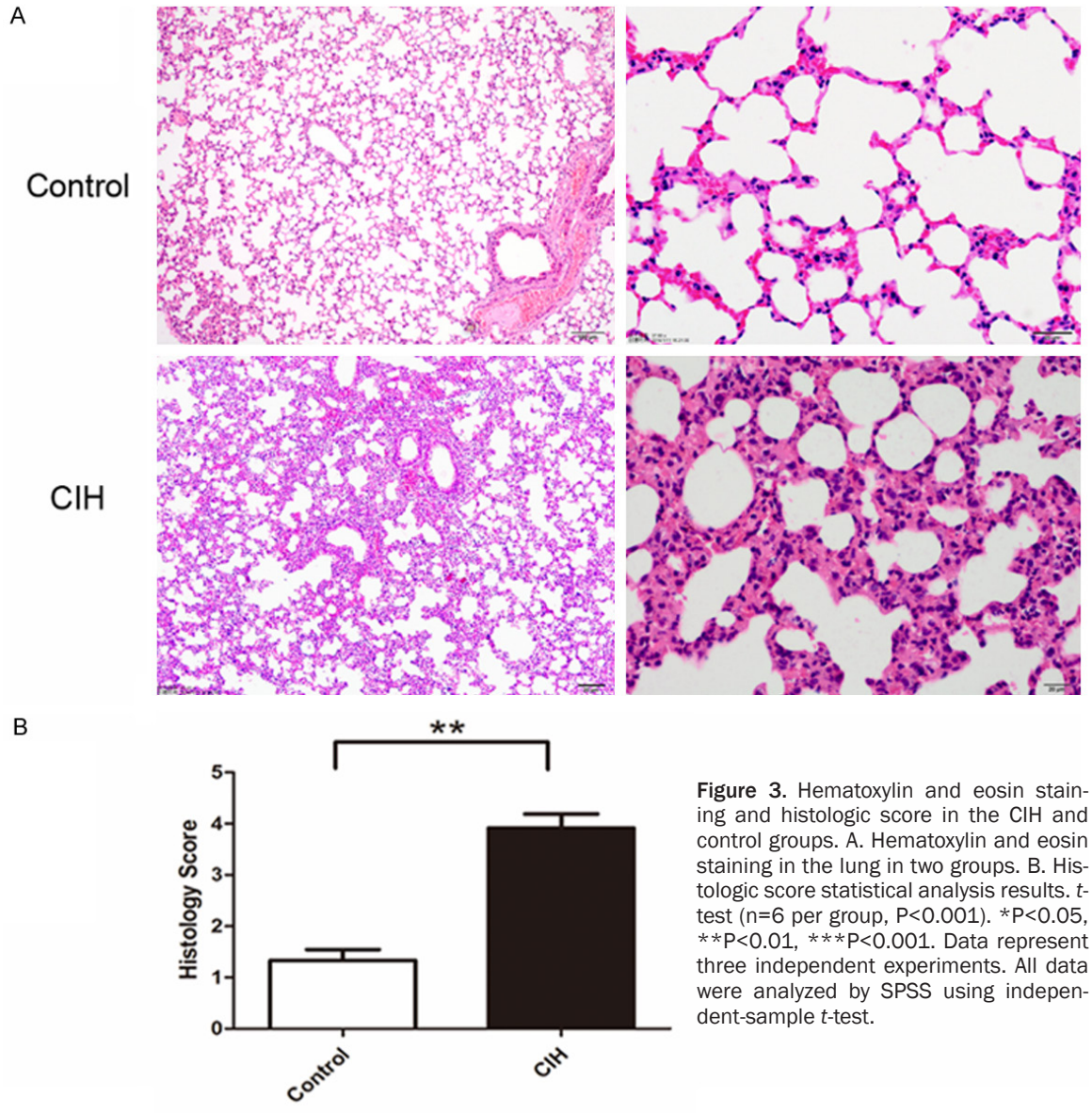

Figure 3. Hematoxylin and eosin staining and histologic score in the CIH and control groups. A. Hematoxylin and eosin staining in the lung in two groups. B. Histologic score statistical analysis results. *t*-test (n=6 per group, P<0.001). *P<0.05, **P<0.01, ***P<0.001. Data represent three independent experiments. All data were analyzed by SPSS using independent-sample *t*-test.

group compared to that in the control group (P<0.01, **Figure 3B**). It indicated thickened lung alveolar walls, increased infiltration of lymphocytes and mononuclear cells, and mild lung congestion in the CIH group compared to the control group.

To investigate the mechanism of decreased pulmonary clearance of PM in mice with intermittent hypoxia, we analyzed gene expression in the lung. Gene expression related to mucin secretion had changed. It was shown that expression of MUC5AC, CXCL1, MIP-2, and Gob5 was higher, and expression of CC16 was lower in the CIH group (**Figure 4**). Gob-5 and MUC5AC appear to be the most prominent representation of mucins, particularly in the pathological state [23, 24]. CXCL1 [25], CC16 [26], and MIP-2 [27] reportedly influenced mucin secretion indirectly. Mucins are the main secretory components of mucus [24]. Therefore, we question the mucus secretion condition in these two groups.

To further evaluate the mucus secretion in the airway, PAS staining was used. Mucus hypersecretion appeared in the small airway in mice with intermittent hypoxia (**Figure 5A**, **5C**), but not in the larger airway (**Figure 5B**). Consistent with the increased messenger RNA expression of MUC5AC in the lung, MUC5AC protein in the bronchoalveolar lavage fluid was also elevated

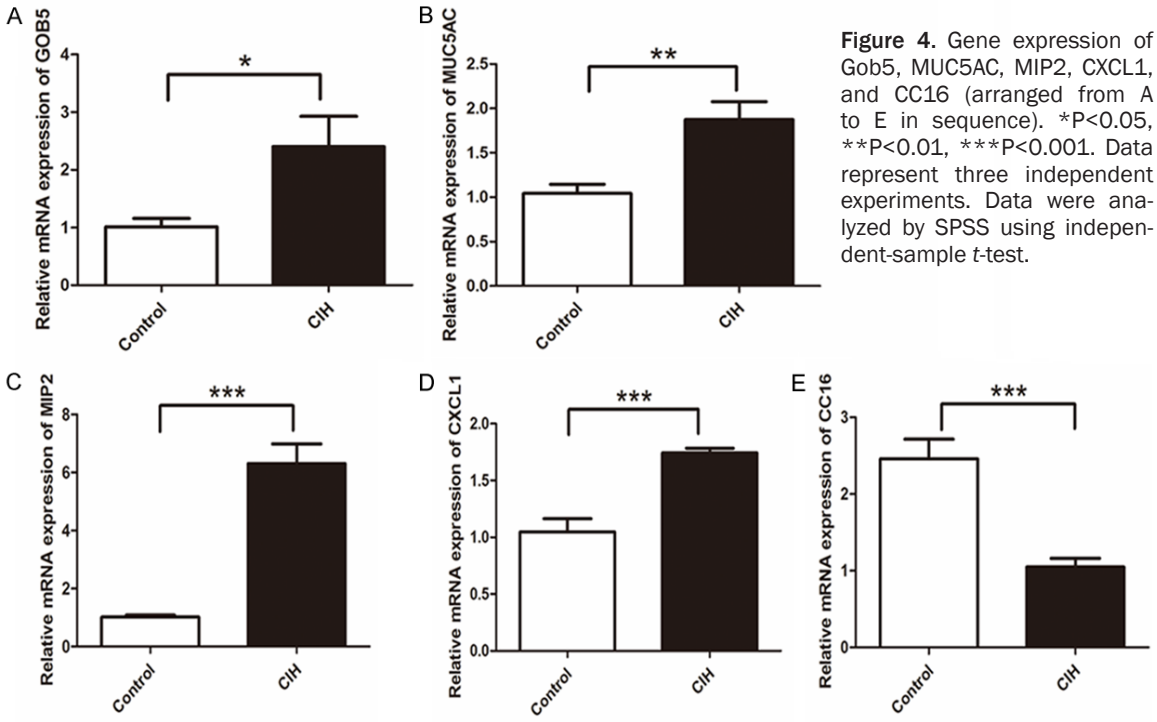

Figure 4. Gene expression of Gob5, MUC5AC, MIP2, CXCL1, and CC16 (arranged from A to E in sequence). *P<0.05, **P<0.01, ***P<0.001. Data represent three independent experiments. Data were analyzed by SPSS using independent-sample *t*-test.

(P<0.05, **Figure 5D**). A standard curve and formula derived from the standard substance is shown in Figure S3. Excessiv e mucus may contribute to the pathogenesis of impaired clearance of PM in mice with CIH.

The role of the PI3K/Akt pathway in intermittent hypoxia

The PI3K/AKT pathway was activated in mice with CIH. Messnger RNA expression of PI3K was significantly higher (**Figure 6B**) and P-PI3K and P-AKT were excessively activated (P<0.05, **Figure 6A**, **6C**, **6D**). This might imply the potential effect of the PI3K/AKT pathway in mucus hypersecretion.

Discussion

Increased PM deposit might be a new pathologic mechanism in patients with OSAHS. It was reported that air pollution exposure has a negative effect on sleep, and there is significant association between exposure to PM and sleep disturbances [28]. Some studies showed the correlation between air pollution and the prevalence of sleep-breath disorders. A significant seasonal pattern was uncovered in the apnea-hypopnea index of different patients undergoing polysomnography, which may be due to environmental aspects of winter [29]. One possible explanation for changes in OSAHS severity may be air pollution, as has been raised on PM-10 [32]. In addition, reduction in air pollution exposure may decrease the severity of respiratory disturbance indices and nocturnal hypoxemia in patients [30]. It is biologically plausible that elevations in ambient pollution might also increase the risk of more clinically relevant sleep-breath disorder and associated oxyhemoglobin desaturation, through effects on upper or lower airway inflammation, autonomic dysfunction, or oxidative stress [31].

Patients with OSAHS had higher mucus levels in the throat [32]. Excessive mucus production is a main factor leading to sleep disturbance, and is just as important as dyspnea and cough. Abundant mucus production may prolong sleep onset, especially because mucus production is exaggerated in the supine position. Airway mucus is a mixture of water, cells, cellular debris, and mucins-heavy glycoproteins-which represent the major protein component of mucus. Mucus secretion functions as a guard and barrier for the airway epithelium. An appropriate amount of mucus secretion traps inhaled PM and transports it out of the lungs by means of ciliary beating and cough, whereas the chronic and hypersecretion of mucus can

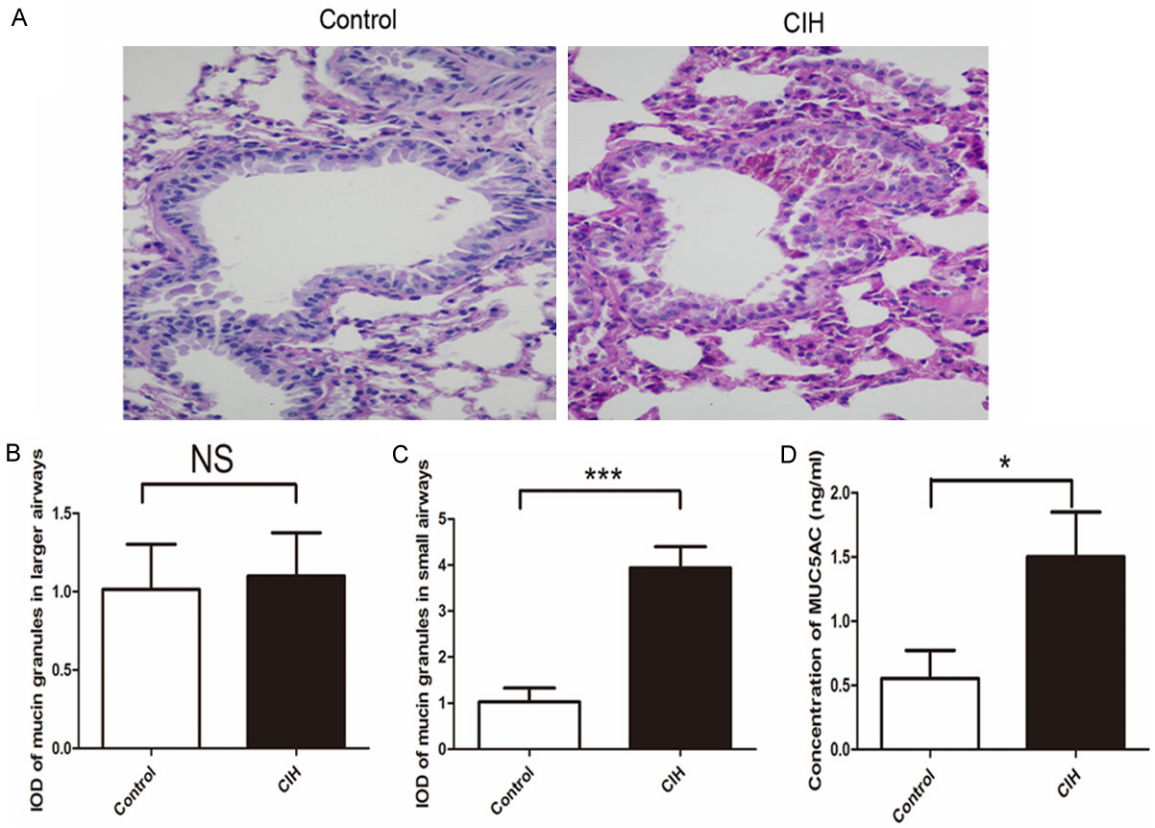

Figure 5. Mucus secretion in mice was analyzed by periodic acid-Schiff (PAS) staining in the lung in these two groups. The left lung lobes were stained with PAS staining. The slides were scanedati 400 × magnifications (A), and the integrated optical density of mucin granules in large (B) and small airways (C), double-blind analysis performed in Image-Pro Plus 6.0. (D) Enzyme-linked immunosorbent assay results of MUC5AC in bronchoalveolar lavage fluid. Concentration of MUC5AC protein in the bronchoalveolar lavage fluid calculated from the standard curve in the same experiments (n=6 per group, $P<0.05$). Data were given as mean ± standard deviation (n=8), *$P<0.05$, **$P<0.01$, ***$P<0.001$. Data represent three independent experiments. All data were analyzed by SPSS using independent-sample *t*-test.

induce severe airway obstruction and repeated airway infection [33]. MUC5AC is the predominant mucin of the human airway and is only secreted in the pathological state [34, 35]. Knockout of MUC5AC attenuated lung inflammation and pulmonary edema during injurious ventilation [36]. Excessive mucus and chronic inflammation contributed to the pathogenesis of common airway diseases and influences the clearance of PM in mice with CIH. In this study, mucus hypersecretion was found in the small airway but not in the larger airway, and might influence the pulmonary clearance ability of mice with CIH.

The upper airway of patients with OSAHS was subjected to recurrent negative pressure swings promoting its collapse and reopening, which could lead to an early local inflammatory process in the upper airway [37, 38]. MIP-2 plays an important role in this upper airway inflammatory process in patients with OSAHS [27]. CC16 is the most abundant protein in normal airway secretions, which maintains the homeostasis of the airway epithelium, and has anti-inflammatory activities in lungs exposed to ozone, allergens, and viruses [26]. Gob5 is a highly induced, putative calcium-activated chloride channel involved in the regulation of mucus production and/or secretion. Gob5 may have a role in fiber clearance in asbestos-associated lung diseases [39]. In addition, we first suggest its activation in PM clearance in mice with intermittent hypoxia. Gob5 has recently been detected in goblet cells within the tracheal and bronchial epithelium amid mucus metaplasia and is implicated in the regulation of mucus secretion by controlling the packaging and/or

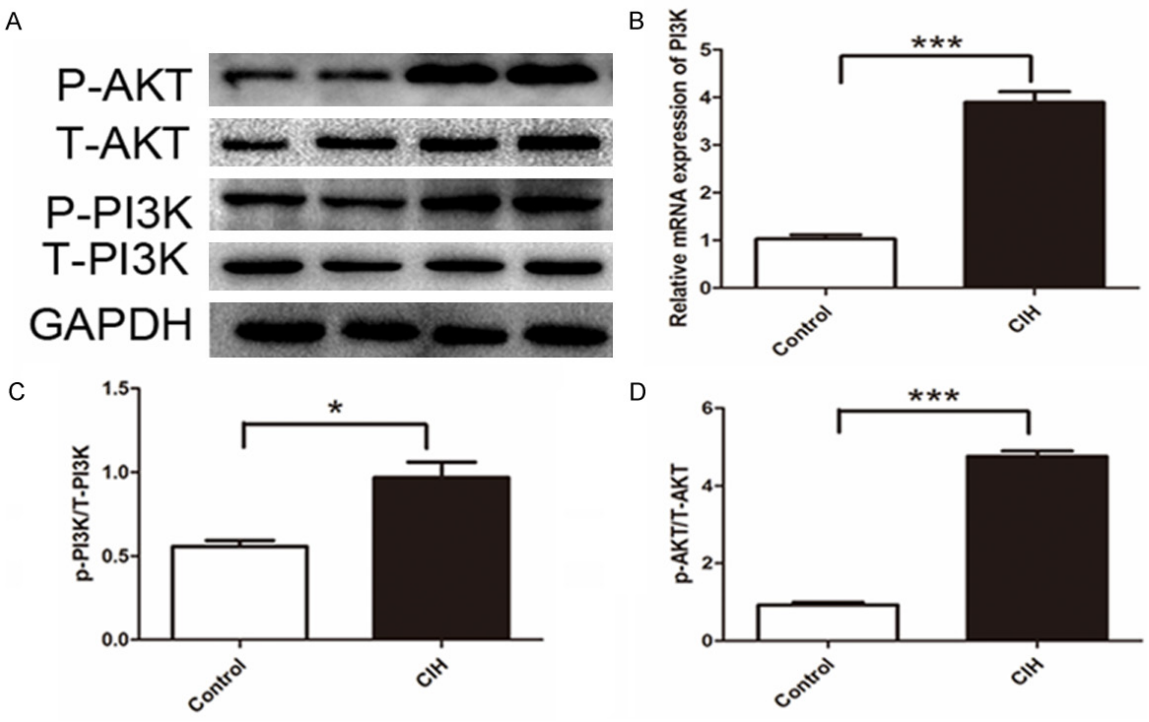

Figure 6. Activation of phosphorylation of PI3K/AKT pathway. A. Western blot bands of target molecular. B. Gene expression of PI3K. C. Intensity of P-PI3K to total PI3K (T-PI3K) P=0.0135. D. Intensity of P-AKT to total AKT (T-AKT) P<0.001. Data represent three independent experiments. All data were analyzed by SPSS using independent-sample *t*-test.

release of secreted mucins like MUC5AC [40]. Furthermore, another explanation is that induced HIF-1 was a consensus-binding motif of all currently sequenced mammalian MUC5AC orthologs [41]. As HIF-1 is increased in intermittent hypoxia as our previous study showed, a critical role for HIF-1 in the regulation of MUC5AC in allergic mucous metaplasia is interesting.

Intermittent hypoxia may destroy mucociliary clearance, amplify mucus production, and result in mucus hypersecretion, decreasing the pulmonary clearance of PM. The mechanisms responsible for the secretion of MUC5AC may result from the activation of excessive activation of phosphorylation of PI3K)/Akt signaling pathway, which was shown to be important in mucus secretion [42]. However, the additional mechanisms responsible for the activation of MUC5AC need to be explored later.

Although there was no direct evidence showing that OSAHS increases airway resistance, initial clinical studies showed that inpatients with OSAHS a decrease in short-term lung function develops after intermittent hypoxic sleep [42]. As was shown previously, the total resistance of the respiratory system was decreased when CIH in patients with OSAHS was corrected [43]. A single night's loss of sleep resulted in significant reductions of forced expiratory volume in 1 second and forced vital capacity in patients [44]. The increase of airway resistance in patients with OSAHS might also correlate with the high prevalence of overlap syndrome with chronic obstructive pulmonary disease [45]. Our study showed that long-term CIH resulted in decreased lung compliance and increased elastic airway resistance and R_L. The value of sRaw could reflect mucin secretion indirectly. It was known that airway hyperresponsiveness resulted in a higher value of sRaw [46]. Mucin secretion from airway cells could influence pulmonary airway hyperresponsiveness and inhibition of mucin secretion from the airway could attenuate pulmonary airway hyperresponsiveness [47]. In this study, higher sRaw value in the CIH group implied pulmonary airway hyperresponsiveness in mice with intermittent hypoxia and might correlate with mucinhypersecretion.

Intermittent hypoxia might destroy mucociliary clearance, amplify mucus production, and result in mucus hypersecretion, decreasing the pulmonary clearance of PM. The mechanisms responsible for the secretion of MUC5AC may result from the activation of excessive activation of phosphorylation of the PI3K/Akt signaling pathway, which was shown to be important in mucus secretion [48]. However, additional mechanisms responsible for the activation of MUC5AC need to be explored later.

In this study, we demonstrated for the first time that intermittent hypoxia decreased the airway clearance of PM in the lung in mice, which might be related to mucus hypersecretion in the small airway rather than the larger airway. Changes in special airway resistance and pulmonary compliance were first raised in mice with intermittent hypoxia in this study. Increase of airway resistance interacted with inflammatory response. There were also limitations that we had not expected, whether the results could be reversed if mucus secretion was decreased using drugs. Additional studies on mucus secretion are needed.

Acknowledgements

This study was supported by National Natural Science Foundation of China (No. 81472175, 81570081, 81400018, 81570028). Authors thank Suchi Chang at Shanghai Medical College, Fudan University for assisting in editing the language.

Disclosure of conflict of interest

None.

Address correspondence to: Dr. Shanqun Li and Jian Zhou, Department of Pulmonary Medicine, Center of Snoring and Sleep Apnea Medicine, Zhongshan Hospital of Fudan University, Fenglin Road 180, Shanghai 200032, China. Tel: 86-18616880856; E-mail: lsq18616880856@163.com (SQL); zhou.jian@fudan.edu.cn (JZ)

References

[1] Poschl U. Atmospheric aerosols: composition, transformation, climate and health effects. Angew Chem Int Ed Engl 2005; 44: 7520-7540.

[2] Shafer MM, Perkins DA, Antkiewicz DS, Stone EA, Quraishi TA and Schauer JJ. Reactive oxygen species activity and chemical speciation of size-fractionated atmospheric particulate matter from Lahore, Pakistan: an important role for transition metals. J Environ Monit 2010; 12: 704-715.

[3] Sforza E and Roche F. Chronic intermittent hypoxia and obstructive sleep apnea: an experimental and clinical approach. Hypoxia (Auckl) 2016; 4: 99-108.

[4] Office on Smoking and Health. Publications and Reports of the Surgeon General. In: editors. The health consequences of involuntary exposure to tobacco smoke: a report of the surgeon general. Atlanta (GA): Centers for Disease Control and Prevention (US); 2006.

[5] Pelayo R and Sivan Y. Increased behavioral morbidity in school-aged children with sleep-disordered breathing. Pediatrics 2005; 116: 797-798; author reply 798.

[6] Menzel DB. The toxicity of air pollution in experimental animals and humans: the role of oxidative stress. Toxicol Lett 1994; 72: 269-277.

[7] Calais CJ, Robertson BD and Beakes DE. Association of allergy/immunology and obstructive sleep apnea. Allergy Asthma Proc 2016; 37: 443-449.

[8] Churg A and Brauer M. Ambient atmospheric particles in the airways of human lungs. Ultrastruct Pathol 2000; 24: 353-361.

[9] Adegunsoye A and Balachandran J. Inflammatory response mechanisms exacerbating hypoxemia in coexistent pulmonary fibrosis and sleep apnea. Mediators Inflamm 2015; 2015: 510105.

[10] Lavie L. Intermittent hypoxia: the culprit of oxidative stress, vascular inflammation and dyslipidemia in obstructive sleep apnea. Expert Rev Respir Med 2008; 2: 75-84.

[11] Sears PR, Yin WN and Ostrowski LE. Continuous mucociliary transport by primary human airway epithelial cells in vitro. Am J Physiol Lung Cell Mol Physiol 2015; 309: L99-108.

[12] Padman R, Geouque DM and Engelhardt MT. Effects of the flutter device on pulmonary function studies among pediatric cystic fibrosis patients. Del Med J 1999; 71: 13-18.

[13] Diogo LN and Monteiro EC. The efficacy of antihypertensive drugs in chronic intermittent hypoxia conditions. Front Physiol 2014; 5: 361.

[14] Fu C, Jiang L, Zhu F, Liu Z, Li W, Jiang H, Ye H, Kushida CA and Li S. Chronic intermittent hypoxia leads to insulin resistance and impaired glucose tolerance through dysregulation of adipokines in non-obese rats. Sleep Breath 2015; 19: 1467-1473.

[15] Wu Y, Kotzer CJ, Makrogiannis S, Logan GA, Haley H, Barnette MS and Sarkar SK. A noninvasive [99mTc]DTPA SPECT/CT imaging meth-

odology as a measure of lung permeability in a guinea pig model of COPD. Mol Imaging Biol 2011; 13: 923-929.
[16] Liu G, Hu Y, Xiao J, Li X, Li Y, Tan H, Zhao Y, Cheng D and Shi H. 99mTc-labelled anti-CD11b SPECT/CT imaging allows detection of plaque destabilization tightly linked to inflammation. Sci Rep 2016; 6: 20900.
[17] Flandre TD, Leroy PL and Desmecht DJ. Effect of somatic growth, strain, and sex on double-chamber plethysmographic respiratory function values in healthy mice. J Appl Physiol (1985) 2003; 94: 1129-1136.
[18] Strope GL, Cox CL, Pimmel RL and Clyde WA Jr. Dynamic respiratory mechanics in intact anesthetized hamsters. J Appl Physiol Respir Environ Exerc Physiol 1980; 49: 197-203.
[19] Amdur MO and Mead J. Mechanics of respiration in unanesthetized guinea pigs. Am J Physiol 1958; 192: 364-368.
[20] Dabbagh K, Takeyama K, Lee HM, Ueki IF, Lausier JA and Nadel JA. IL-4 induces mucin gene expression and goblet cell metaplasia in vitro and in vivo. J Immunol 1999; 162: 6233-6237.
[21] Su X, Bai C, Hong Q, Zhu D, He L, Wu J, Ding F, Fang X and Matthay MA. Effect of continuous hemofiltration on hemodynamics, lung inflammation and pulmonary edema in a canine model of acute lung injury. Intensive Care Med 2003; 29: 2034-2042.
[22] Chen H, Wu G, Sun Q, Dong Y and Zhao H. Hyperbaric oxygen protects mandibular condylar chondrocytes from interleukin-1beta-induced apoptosis via the PI3K/AKT signaling pathway. Am J Transl Res 2016; 8: 5108-5117.
[23] Sabo-Attwood T, Ramos-Nino M, Bond J, Butnor KJ, Heintz N, Gruber AD, Steele C, Taatjes DJ, Vacek P and Mossman BT. Gene expression profiles reveal increased mClca3 (Gob5) expression and mucin production in a murine model of asbestos-induced fibrogenesis. Am J Pathol 2005; 167: 1243-1256.
[24] Evans CM, Kim K, Tuvim MJ and Dickey BF. Mucus hypersecretion in asthma: causes and effects. Curr Opin Pulm Med 2009; 15: 4-11.
[25] Muller HD, Cvikl B, Lussi A and Gruber R. Chemokine expression of oral fibroblasts and epithelial cells in response to artificial saliva. Clin Oral Investig 2016; 20: 1035-1042.
[26] Laucho-Contreras ME, Polverino F, Gupta K, Taylor KL, Kelly E, Pinto-Plata V, Divo M, Ashfaq N, Petersen H, Stripp B, Pilon AL, Tesfaigzi Y, Celli BR and Owen CA. Protective role for club cell secretory protein-16 (CC16) in the development of COPD. Eur Respir J 2015; 45: 1544-1556.
[27] Wagner JG, Birmingham NP, Jackson-Humbles D, Jiang Q, Harkema JR and Peden DB. Supplementation with gamma-tocopherol attenuates endotoxin-induced airway neutrophil and mucous cell responses in rats. Free Radic Biol Med 2014; 68: 101-109.
[28] Abou-Khadra MK. Association between PM(1) (0) exposure and sleep of Egyptian school children. Sleep Breath 2013; 17: 653-657.
[29] Cassol CM, Martinez D, da Silva FA, Fischer MK, Lenz Mdo C and Bos AJ. Is sleep apnea a winter disease?: meteorologic and sleep laboratory evidence collected over 1 decade. Chest 2012; 142: 1499-1507.
[30] Zanobetti A, Redline S, Schwartz J, Rosen D, Patel S, O'Connor GT, Lebowitz M, Coull BA and Gold DR. Associations of PM10 with sleep and sleep-disordered breathing in adults from seven U.S. urban areas. Am J Respir Crit Care Med 2010; 182: 819-825.
[31] Liu WT, Lee KY, Lee HC, Chuang HC, Wu D, Juang JN and Chuang KJ. The association of annual air pollution exposure with blood pressure among patients with sleep-disordered breathing. Sci Total Environ 2016; 543: 61-66.
[32] Kreivi HR, Virkkula P, Lehto J and Brander P. Frequency of upper airway symptoms before and during continuous positive airway pressure treatment in patients with obstructive sleep apnea syndrome. Respiration 2010; 80: 488-494.
[33] Faderl M, Noti M, Corazza N and Mueller C. Keeping bugs in check: the mucus layer as a critical component in maintaining intestinal homeostasis. IUBMB Life 2015; 67: 275-285.
[34] Rose MC and Voynow JA. Respiratory tract mucin genes and mucin glycoproteins in health and disease. Physiol Rev 2006; 86: 245-278.
[35] Evans CM and Koo JS. Airway mucus: the good, the bad, the sticky. Pharmacol Ther 2009; 121: 332-348.
[36] Livraghi-Butrico A, Grubb BR, Wilkinson KJ, Volmer AS, Burns KA, Evans CM, O'Neal WK and Boucher RC. Contribution of mucus concentration and secreted mucins Muc5ac and Muc5b to the pathogenesis of muco-obstructive lung disease. Mucosal Immunol 2017; 10: 395-407.
[37] Almendros I, Carreras A, Ramirez J, Montserrat JM, Navajas D and Farre R. Upper airway collapse and reopening induce inflammation in a sleep apnoea model. Eur Respir J 2008; 32: 399-404.
[38] Kitaoka H, Doi Y, Casey SA, Hitomi N, Furuno T and Maron BJ. Comparison of prevalence of apical hypertrophic cardiomyopathy in Japan and the United States. Am J Cardiol 2003; 92: 1183-1186.
[39] Mossman BT. In vitro studies on the biologic effects of fibers: correlation with in vivo bioassays. Environ Health Perspect 1990; 88: 319-322.

[40] Zhou Y, Shapiro M, Dong Q, Louahed J, Weiss C, Wan S, Chen Q, Dragwa C, Savio D, Huang M, Fuller C, Tomer Y, Nicolaides NC, McLane M and Levitt RC. A calcium-activated chloride channel blocker inhibits goblet cell metaplasia and mucus overproduction. Novartis Found Symp 2002; 248: 150-165; discussion 165-170, 277-182.

[41] Young HW, Williams OW, Chandra D, Bellinghausen LK, Perez G, Suarez A, Tuvim MJ, Roy MG, Alexander SN, Moghaddam SJ, Adachi R, Blackburn MR, Dickey BF and Evans CM. Central role of Muc5ac expression in mucous metaplasia and its regulation by conserved 5' elements. Am J Respir Cell Mol Biol 2007; 37: 273-290.

[42] Kunos L, Lazar Z, Martinovszky F, Tarnoki AD, Tarnoki DL, Kovacs D, Forgo B, Horvath P, Losonczy G and Bikov A. Overnight changes in lung function of obese patients with obstructive sleep apnoea. Lung 2017; 195: 127-133.

[43] Kita H, Ohi M, Chin K, Noguchi T, Otsuka N, Tsuboi T and Kuno K. Effects of nasal continuous positive airway pressure therapy on respiratory parameters of upper airway patency in patients with obstructive sleep apnea syndrome. Chest 1998; 114: 691-696.

[44] Kleisiaris CF, Kritsotakis EI, Daniil Z, Tzanakis N, Papaioannou A and Gourgoulianis KI. The prevalence of obstructive sleep apnea-hypopnea syndrome-related symptoms and their relation to airflow limitation in an elderly population receiving home care. Int J Chron Obstruct Pulmon Dis 2014; 9: 1111-1117.

[45] Soler X and Gaio E. High prevalence of obstructive sleep apnea in patients with moderate to severe chronic obstructive pulmonary disease. Ann Am Thorac Soc 2015; 12: 1219-1225.

[46] Lomask M. Further exploration of the Penh parameter. Exp Toxicol Pathol 2006; 57 Suppl 2: 13-20.

[47] Agrawal A, Singh SK, Singh VP, Murphy E and Parikh I. Partitioning of nasal and pulmonary resistance changes during noninvasive plethysmography in mice. J Appl Physiol (1985) 2008; 105: 1975-1979.

[48] Yu Q, Chen X, Fang X, Chen Q and Hu C. Caveolin-1 aggravates cigarette smoke extract-induced MUC5AC secretion in human airway epithelial cells. Int J Mol Med 2015; 35: 1435-1442.